

Lattice Melting in Perpetually Pulsating Equilibria

Pichon, Christophe^a & Lynden-Bell Donald^b

^a *Institut d'Astrophysique de Paris UMR 7595 UPMC, 98 bis boulevard d'Arago, 75014 Paris, France*

^b *Institute of Astronomy and Clare College, Madingley Road, Cambridge CB3 0HA, UK*

Abstract

Systems whose potential energies consists of pieces that scale as r^{-2} together with pieces that scale as r^2 , show no violent relaxation to Virial equilibrium but may pulsate at considerable amplitude for ever. Despite this pulsation these systems form lattices when the non-pulsational energy is low, and these disintegrate as that energy is increased. The quasi specific heats show the expected halving as the 'solid' is gradually replaced by the gas of independent particles. The forms of the lattices are described here for $N \leq 20$ while they become hexagonal close packed for large N . In the larger N limit, a shell structure is formed. Their large N behaviour is analogous to a $\gamma = 5/3$ polytropic gas with a quasi-gravity such that every element of fluid attracts every other in proportion to their separation.

Résumé

Fusion de réseaux en équilibre d'oscillations perpétuelles Les systèmes dont l'énergie potentielle est constituée d'une composante en r^{-2} et d'une composante en r^2 ne présentent pas de relaxation violente vers l'équilibre du viriel mais vont osciller fortement indéfiniment. En dépit de ces pulsations, de tels systèmes forment un réseau quand l'énergie non oscillatoire reste faible, et se désintègrent si elle augmente. Leurs quasi chaleur spécifique est divisée par deux quand le gaz de particules indépendantes remplace la phase solide. La forme du crystal est décrite ici pour $N \leq 20$. Dans la limite des grands N le réseau se stratifie en coquilles suivant un motif hexagonal compact.

Key words: gravitation, statistical mechanics, phase transition

5	Two hexagons joined on a face
6	Two pyramids joined at their base
7	Two pentagonal pyramids joined at their base
8	A twisted cube
9	Three pyramids sharing the edge of a base
10	Two twisted pyramids
11	Two twisted pyramids and one center
12	Isocahedron i.e. two skewed pentagonal pyramids
13	Isocahedron and one center
14	Hexagonal and pentagonal pyramid and one center
15	Two skewed hexagonal pyramid and one center
16	Pentagonal pyramid and an hexagon and a triangle and one center
17	Hexagonal pyramid over an hexagon over a triangle and one center
18	Two pentagonal pyramid and one twisted pentagon and one center

Table 1

First 18 configurations of equilibria. A few of them are shown on Figure 1. Note that as the number of elements increases, the final configurations need not be unique.

1 Introduction

Astrophysics has provided several new insights into ways statistical mechanics may be extended to cover a wider range of phenomena. Negative heat capacity, bodies which get cooler when you heat them, were first encountered by Eddington (1916) and when such bodies were treated thermodynamically by Lynden-Bell & Wood (1968), what seemed natural to astronomers was seen as an apparent contradiction in basic physics to those from statistical mechanics background. Even after a physicist Thirring (1970) first resolved this paradox and Lynden-Bell & Lynden-Bell (1977) gave an easily soluble example, there was considerable reluctance to accept the idea that micro canonical ensembles could give such different results to canonical ones. Nevertheless, there was still some reluctance even in 1999 Lynden-Bell (D), though to those working on simulations of small clusters of atoms or molecules, the distinction was well understood by the early 1990s, see *e.g.* Wales (2001). However by 2005, the broader statistical mechanics community had embraced these ideas, and emphasized this difference which had been with us for 30 years. Another area to which statistical mechanics might extend is that of collisionless systems which may be treated as “Vlasov” fluids in phase space. While early attempts at

Email address: `pichon@iap.fr` (Pichon, Christophe).

finding such equilibria gave interesting formulae reminiscent of a Fermi-Dirac distribution Lynden-Bell (1967), there is ample evidence from astronomical simulations that these equilibria are not reached in gravitational systems. There are also different ways of doing the counting that lead to different results and recently, Arad I. (2005) gave an example that demonstrates that the concept of a unique final state determined by a few constants of motion found from the initial state is not realized. Thus the statistical mechanics of fluids in phase space remains poorly understood with theory at best loosely correlated with simulations and experiments.

This paper is concerned with a third area of non standard statistical mechanics which is restricted to very special systems, those for which the oscillation of the system separates off dynamically from the behaviour of the rescaled variables that are now scale free. These systems were found as a bi-product of a study which aimed at generalizing Newton's soluble N-body problem Lynden-Bell & Lynden-Bell (1999a) (paper I) and a first skimish with the statistical dynamics of the scale free variables despite the continuing oscillation of the scale was given there. Since then, Lynden-Bell & Lynden-Bell (2004), hereafter paper III, have showed that the peculiar velocities of the particles do indeed relax, as predicted, to a Maxwellian distribution, whose temperature continuously change as $(\text{scale})^{-2}$. This occurs, whatever the ratio of the relaxation time to the pulsation period. The peculiar velocities are larger whenever the system is smaller. The interest of this problem for those versed in statistical mechanics is that there is no longer an energy that is shared between the different components of motions. The interest for astronomers lies in part because these systems suffer no violent relaxation to a size that obeys the Virial theorem. Nevertheless, despite the continual pulsation of such systems the rescaled variables within them do relax to a definite equilibrium.

In this paper, we demonstrate that such systems can form solids (albeit ones that pulsate in scale). We study in Section 3 their behaviour in the large N limits and show that they stratify into shells. By appealing to an analogy with a $\gamma = 5/3$ gaseous system, we predict their equilibrium configuration and investigate their properties. We also study the phase transition as these structures melt and the corresponding changes in "specific heat". Section 2 derives the basic formulae for the N-body system and its gaseous analog.

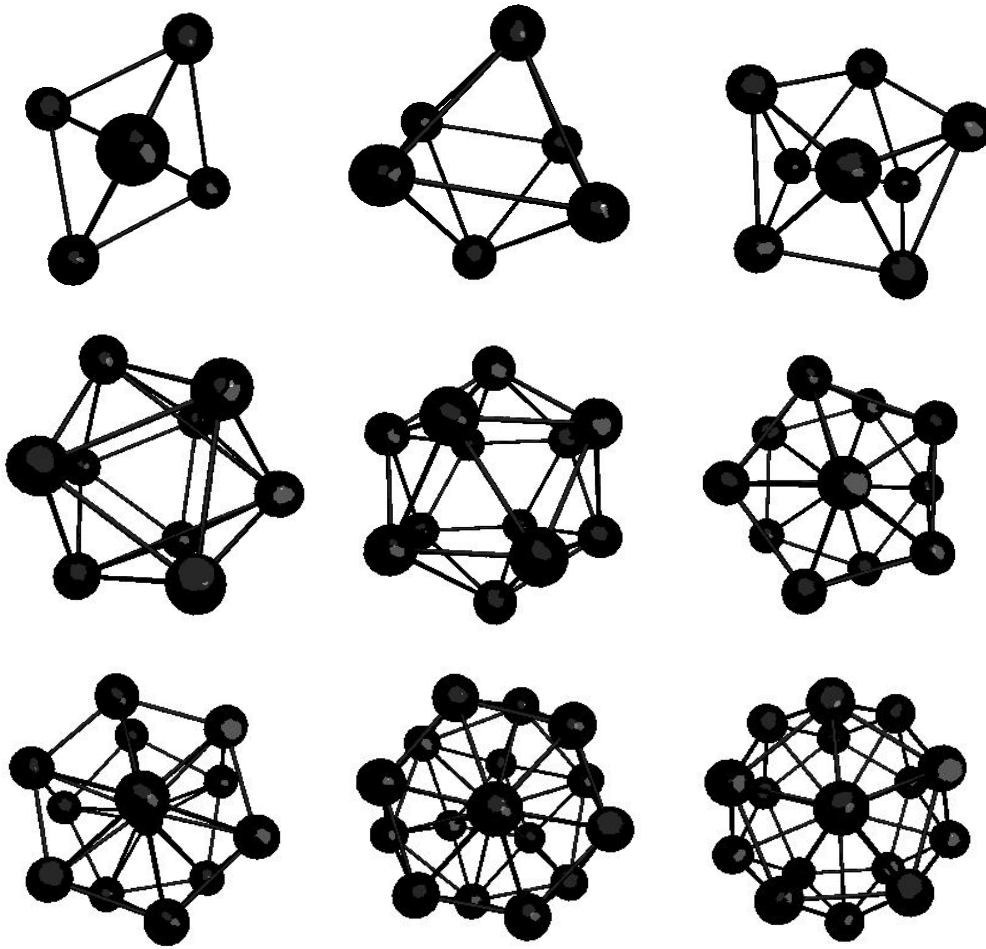


Fig. 1. A few set of remarkable equilibria; for left to right and top to bottom: $n = [5]$ two hexagons joined by basis, $[6]$ two pyramids joined by basis, $[8]$ two twisted squares, $[12]$ isocahedron i.e. two skewed pentagonal pyramid, $[13]$ isocahedron+center, $[14]$ hexagonal+ pentagonal pyramid+center, $[17]$ hexagonal pyramid over hexagon over triangle+center, $[18]$ two pentagonal pyramid+twisted pentagon center

2 Derivation

2.1 The discrete system

We consider N particles of masses m_i at \mathbf{r}_i , $i = N$ and set

$$\sum m_i = M, \quad \sum m_i \mathbf{r}_i = M \bar{\mathbf{r}}, \quad (1)$$

and

$$I = \sum m_i (\mathbf{r}_i - \bar{\mathbf{r}})^2 = Ma^2. \quad (2)$$

In earlier work we showed both classically (paper I) and quantum mechanically Lynden-Bell & Lynden-Bell (1999b) (paper II) that if the potential energy of the whole system was of the form

$$V = W(a) + a^{-2}W_2(\hat{\mathbf{a}}), \quad (3)$$

where $\hat{\mathbf{a}}$ is the 3N dimensional unit vector

$$\hat{\mathbf{a}} = \frac{N^{-1/2}}{a}(\mathbf{r}_1 - \bar{\mathbf{r}}, \mathbf{r}_2 - \bar{\mathbf{r}} \dots, \mathbf{r}_N - \bar{\mathbf{r}}), \quad (4)$$

then the motion of the scaling variable r separates dynamically from the motions of both $\bar{\mathbf{r}}$ and the $\hat{\mathbf{r}}$ so those motions decouple. If we ask that V be made up of a sum of pairwise interactions then we need

$$W = \frac{1}{2}\omega^2 M a^2 = V_{-2}, \quad (5)$$

where ω^2 is constant, and

$$a^{-2}W_2(\hat{\mathbf{a}}) = V_2 = \sum_{i < j} \sum K_2 |r_i - r_j|^{-2}. \quad (6)$$

Let us now see why potentials of the for $V_2 + V_{-2}$ are so special by looking at the Virial Theorem and the condition of Energy conservation. Take the more general potential energy to be a sum of pieces V_n where each V_n scales as r^{-n} on a uniform expansion. n can be positive or negative. Then $V = \sum V_n$. For such a system the Virial Theorem reads:

$$\frac{1}{2}\ddot{I} = 2T + \sum nV_n = 2E + \sum (n - 2)V_n .$$

Now we already saw that $V_{-2} \propto I$ and V_2 clearly drops out of the final sum because $n - 2$ is zero. Thus for potentials of the form $V = V_{-2} + V_2$

$$\frac{1}{2}\ddot{I} = 2E - 4V_{-2} = 2E - 4\omega^2 \left(\frac{1}{2}I\right), \quad (7)$$

so I vibrates harmonically with angular frequency 2ω about a mean value E/ω^2 and shows no Violent Relaxation (1). Multiplying by $4\dot{I}$ and integrating

$$\dot{I}^2 = 8EI - 4\omega^2 I^2 - 4M^2 \mathcal{L}^2,$$

where the last term is the constant of integration chosen in conformity with Eq. (8). Now recall from Eq. (2) that $I = Ma^2$ so we find on division by $8M^2a^2$ that

$$\frac{\dot{a}^2}{2} + \frac{\mathcal{L}^2}{2a^2} + \frac{1}{2}\omega^2a^2 = \frac{E}{M}, \quad (8)$$

which we recognise as the specific energy of a particle with specific ‘‘angular momentum’’ \mathcal{L} moving in a simple harmonic spherical potential of ‘frequency’ ω . In such a potential r vibrates about its mean at ‘frequency’ 2ω .

Note here that the $\gamma = 5/3$ gas has a term $3(\gamma-1)U = 2U$ in the virial theorem since its internal energy, U , scales like r^{-2} so it can be likewise absorbed into the total energy term. Thus if every elementary mass of such a gas attracted every other with a force linearly proportional to their separation, then that system too would pulsate eternally, as described above in Eq. (7).

The aim of this paper is to demonstrate the existence of perpetually pulsating equilibrium lattices and to study the changes as the non-pulsational ‘energy’ $M\mathcal{L}^2/2$ is increased. We show that the part of the potential left in the equation of motion for the rescaled variables is the purely repulsive V_2 . It is then not surprising that the lattice disruption at higher non-pulsational energy occurs quite smoothly without any latent heat and the solid phase appears to give way to the gaseous phase of half the specific heat without the appearance of a liquid with another phase transition. The hard sphere solid has been well studied and behaves rather similarly.

2.1.1 *The Equations of Motion and their separation*

Although the work of this section can be carried out when the masses m_i are different, (see paper I), we here save writing by taking $m_i = m$ and so $M = Nm$. We start with V of the form (3). The equations of motion are

$$m\ddot{\mathbf{r}}_i = -\partial V/\partial \mathbf{r}_i \quad . \quad (9)$$

Now V is a mutual potential energy involving only $\mathbf{r}_i - \mathbf{r}_j$ so $\sum_i \partial V/\partial \mathbf{r}_i = 0$ and summing the above equation for all i we have

$$d^2\bar{\mathbf{r}}/dt^2 = 0 \quad , \quad \bar{\mathbf{r}} = \bar{\mathbf{r}}_0 + \mathbf{u}t \quad .$$

Henceforth we shall remove the centre of mass motion and fix the centre of mass at the origin so $\bar{\mathbf{r}} = 0$. Now the $3N$ -vector \mathbf{a} can be rewritten in terms

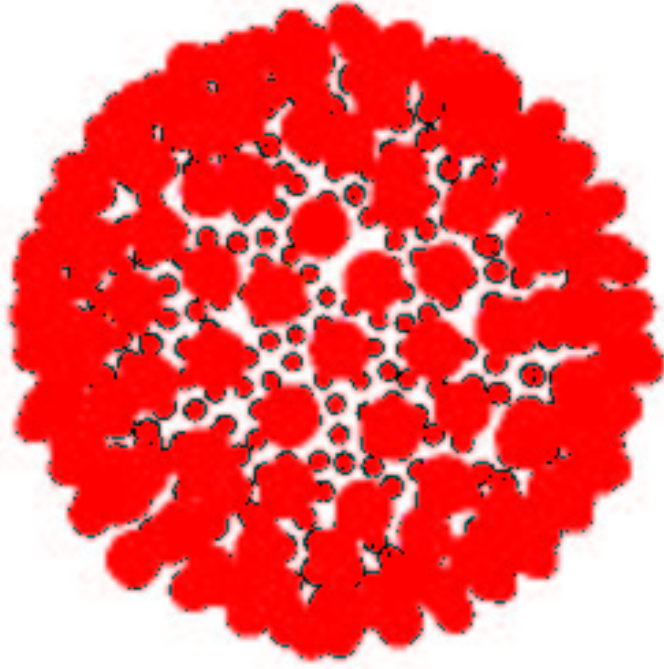


Fig. 2. An example of large N static spherical equilibrium obeying Eq. (9); here only a given shell is represented for clarity.

of its length a and its direction $\hat{\mathbf{a}}$ (a unit vector). Equation (9) takes the form

$$m\ddot{\mathbf{a}} = -\partial V/\partial \mathbf{a} = -W'\hat{\mathbf{a}} + 2r^{-3}W_2\hat{\mathbf{a}} - a^{-3}\partial W_2/\partial \hat{\mathbf{a}}, \quad (10)$$

where we have used the form (3) for V . Notice that when W_2 is zero (or negligibly weak) all the hyperangular momenta of the form $m(r_\alpha \dot{r}_\beta - r_\beta \dot{r}_\alpha)$ (the components of \mathcal{L}) where $\alpha \neq \beta$ run from 1 to $3N$, are conserved!

Taking the dot product of (10) with $N\mathbf{a}$ eliminates the $\partial W_2/\partial \hat{\mathbf{a}}$ term which is purely transverse so we get the Virial Theorem in the form:

$$\frac{1}{2} \frac{d^2}{dt^2}(Ma^2) = M\dot{\mathbf{a}}^2 - a \frac{dW}{da} - 2a^{-2}W_2 = 2E - \frac{1}{a} \frac{d}{da}(a^2W). \quad (11)$$

Multiplying by $\frac{1}{2}d(a^2)/dt$ and integrating Eq. (11) yields

$$\frac{1}{2}Ma^2\dot{a}^2 = Ea^2 - Wa^2 - \frac{1}{2}M\mathcal{L}^2,$$

where the final term is the constant of integration. On division by a^2

$$\frac{M}{2} \left(\dot{a}^2 + \frac{\mathcal{L}^2}{a^2} \right) + W(a) = E, \quad (12)$$

which is the energy equation of a particle of mass M moving with “angular momentum” \mathcal{L} and energy E in a hyperspherical potential $W(a)$. Now

$$\ddot{\mathbf{a}} = \frac{d}{dt}(\dot{a}\hat{\mathbf{a}} + a\dot{\hat{\mathbf{a}}}) = \ddot{a}\hat{\mathbf{a}} + \frac{1}{a}\frac{d}{dt}(a^2\dot{\hat{\mathbf{a}}}) \quad (13)$$

and from (12)

$$\ddot{a} = \frac{\mathcal{L}^2}{a^3} - \frac{1}{M}W'(a) \quad . \quad (14)$$

Inserting these values for \ddot{a} and $\ddot{\mathbf{a}}$ into equation (10) we obtain on simplification, multiplying by a^3 ;

$$Ma^2\frac{d}{dt}\left(a^2\frac{d\hat{\mathbf{a}}}{dt}\right) = 2W_2\hat{\mathbf{a}} - \partial W_2/\partial\hat{\mathbf{a}} - M\mathcal{L}^2\hat{\mathbf{a}} \quad . \quad (15)$$

On writing $d/d\tau = a^2d/dt$ this becomes an autonomous equation for $\hat{\mathbf{a}}(\tau)$. Since $(\dot{\mathbf{a}})^2 = (a\dot{\hat{\mathbf{a}}} + \hat{\mathbf{a}}\dot{a})^2 = a^2\dot{\hat{\mathbf{a}}}^2 + \dot{a}^2$ we may write the energy in the form

$$E = \frac{1}{2}M\left[\frac{1}{a^2}\left(\frac{d\hat{\mathbf{a}}}{d\tau}\right)^2 + \dot{a}^2\right] + V = \frac{1}{2}M\left(\dot{a}^2 + \frac{\mathcal{L}^2}{a^2}\right) + W \quad ,$$

so

$$\frac{1}{2}M\left(\frac{d\hat{\mathbf{a}}}{d\tau}\right)^2 + W_2 = \frac{1}{2}M\mathcal{L}^2 \quad . \quad (16)$$

This shows that the only ‘potential’ in the hyper angular coordinates’ motion is $W_2(\hat{\mathbf{a}})$ and that the effective hyper angular energy in that motion is $\frac{1}{2}M\mathcal{L}^2$ (which has the dimension of a^2 times an energy). In fact we showed in paper I and III that it was this quantity that was equally shared among the hyperangular momenta in the statistical mechanics of perpetually pulsating systems. Subtracting the radial part of (15) from it gives the equation of motion for $\hat{\mathbf{r}}$. The radial part reduces to the $d/d\tau$ derivative of equation (16).

In terms of the true velocities $\mathbf{v}_1, \mathbf{v}_2$ etc

$$\frac{d\hat{\mathbf{a}}}{d\tau} = a^2\frac{d}{dt}\left(\frac{\mathbf{r}_1}{a}, \frac{\mathbf{r}_2}{a} \dots \frac{\mathbf{r}_N}{a}\right) = a\left(\mathbf{v}_1 - \frac{\dot{a}}{a}\mathbf{r}_1, \mathbf{v}_2 - \frac{\dot{a}}{a}\mathbf{r}_2 \text{ etc}\right) \quad ,$$

so it is the peculiar velocities after removal of the Hubble flow $\dot{a}\mathbf{r}_i/a$ and after multiplication by a that constitute the kinetic components of the shared angular energy in the angular potential $W_2(\hat{\mathbf{a}})$.

When the $\frac{1}{2}m(d\hat{\mathbf{a}}/d\tau)^2$ are large enough to escape the potential wells offered by W_2/N we get an almost free particle angular motion of these $3N - 4$ components. The -4 accounts for the fixing of the centre of mass and the removal of $\dot{\mathbf{a}}$ from the kinetic components. If we impose also a prescribed total angular momentum, the number of independent kinetic components would reduce by a further two transverse components to $3N - 6$. However the peculiar velocities are then measured relative to a frame rotating with angular velocity $\tilde{\boldsymbol{\Omega}} \times \mathbf{a}$ where $\tilde{\boldsymbol{\Omega}} = \mathcal{I}^{-1} \cdot \mathbf{J}$. The constant Lagrange multiplier is no longer $\tilde{\boldsymbol{\Omega}}$ but is proportional to a^{-2} since the inertial tensor, \mathcal{I} has that dependence in pulsating equilibrium. The Lagrange multiplier is $\boldsymbol{\Omega} = \tilde{\boldsymbol{\Omega}}a^2$ which is constant during the pulsation and the peculiar velocity is $\mathbf{v}_{\text{pi}} = (\mathbf{v}_i - \mathbf{u}_i)$ where $\mathbf{u}_i = (\dot{\mathbf{a}}\mathbf{r}_i/a + \boldsymbol{\Omega} \times \mathbf{r}_i/a^2)$ see paper III equation (17).¹ Hereafter we specialise to the requirements given by Eq. (5) and (6).

2.2 The $\gamma = 5/3$ analogous gaseous system

When particles attract with both a long range force such as gravity or our linear law of attraction, and a short range repulsion, the latter acts like the pressure of a gas. Indeed short range repulsion forces only extend over a local region, and for large N their effect can be considered as pressure since only the particles close to any surface drawn through the configuration affect the exchange of momentum across that surface. In our case, the local r_{ij}^{-3} forces come from the r_{ij}^{-2} potential which scale as r^{-2} . A barotropic gas with $p = \rho^\gamma$ has an internal energy that behaves as $\rho^{\gamma-1}$ scaling like $r^{-3(\gamma-1)}$. The required r^{-2} scaling gives a γ of $5/3$. Thus we may expect strong *analogies* between a $\gamma = 5/3$ gas with linear long range attraction and our large N particle systems. However an r_{ij}^{-3} repulsion between particles is not of very short range so that the gas is not exactly the same as the large N limit of the particle system. The particle equilibria have the inverse cubic repulsion between particles balancing the long range linear attraction, which can be exactly replaced by a linear attraction to the barycentre proportional to the total mass. For the gas, it is the pressure that balances this long range force.

2.2.1 Mass profile of the static fluid

The equilibrium of such a gas in the presence of a long range force, $-G^*Mr$, (where $MG^* \equiv \omega^2$) is given by

$$\frac{1}{\rho} \frac{dp}{dr} = -G^*Mr. \quad (17)$$

¹ The above definition of \mathbf{u} is correct. That given under equation (18) of paper III has $-\boldsymbol{\Omega}$ for $\boldsymbol{\Omega}$ in error as may be seen from equation (17).

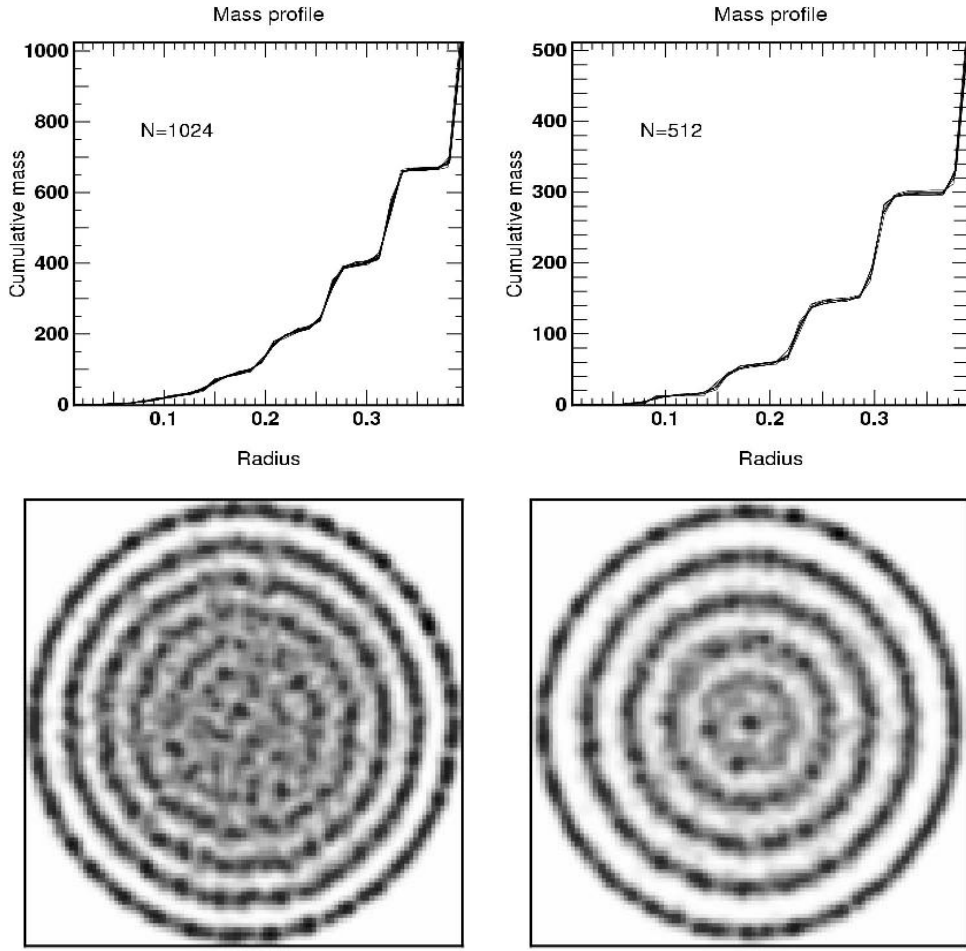


Fig. 3. Mean mass profile and section through a $N = 1024$ and $N = 512$ crystal; The mass profile is derived while stacking different realisations of the lattice and binning the corresponding density. The shell structure is clearly apparent on these figures.

Setting $p = \kappa\rho^{5/3}$, with $\xi \equiv r/r_m$, this yields

$$\rho = \rho_0(1 - \xi^2)^{3/2}, \quad (18)$$

where \mathbf{r} is from now on the 3D configuration space vector measured from the centre of mass of the system and r its modulus, with r_m its value at the edge.

Integrating the density predicts a mass profile, $M(\xi)$,

$$M(\xi) = \frac{\pi M}{12} \left(3 \arcsin(\xi) - \xi(8\xi^4 - 14\xi + 3)\sqrt{1 - \xi^2} \right), \quad (19)$$

and M is the total mass. In practice for the discrete system of Section 2.1, there is a marked layering at equilibrium, and the “pressure” and the mass

profiles depart from their predicted profiles as each monolayers of particles is crossed. See Section 3 and Fig. (3).

The relationship between the polytropic coefficient, κ , and K_2 , the strength of the repulsion (entering W_2 in Eq. (6)) is found by identifying the internal energy of the corresponding gas to the potential energy of the $1/r_{ij}^2$ coupling. In short, the former reads for a $\gamma = 5/3$ fluid with density profile Eq. (17):

$$V_2 = - \int_0^{r_m} \frac{\kappa\gamma}{\gamma-1} \rho^{2/3} 4\pi r^2 \rho dr = - \frac{25\pi^2}{128} \kappa \rho_0^{5/3} r_m^3, \quad (20)$$

while the latter reads:

$$V_2 = - \frac{K_2}{2} \iiint_0^{r_m} \frac{4\pi r^2 \rho(r) 4\pi r'^2 \rho(r') d\mu dr dr'}{r^2 + r'^2 - 2\mu r r'} = - \frac{9\pi^4}{640} \rho_0^2 r_m^4 K_2. \quad (21)$$

Identifying Eq. (20) and (21) gives (using $M = \rho_0 r_m^3 \pi^2/8$)

$$\kappa = \frac{18}{125} \pi^{4/3} M^{1/3} K_2. \quad (22)$$

3 Applications: crystalline forms of pulsating equilibria

Let us now study the discrete form of rotating pulsating equilibria that the systems described in Section 2. Let us first ask ourselves what would the final state of equilibrium in which N particles obeying Eq. (9) would collapse to, if one adds a small drag force in order to damp the motions.

3.1 Numerical setup

A softening scale, s , of 0.05 was used so that the effective interaction potential reads

$$\psi_{12} = \frac{r_{12}^2}{2} + \frac{1}{r_{12}^2 + s^2}, \quad (23)$$

having rescaled both the repulsive and the attractive component of the potential to one by choosing appropriately the time units and the scale units. We computed the total energy of the cluster, together with the invariant, $m\mathcal{L}^2/2$. The relaxation towards the equilibrium should be relatively smooth in order

to favor that the system collapses into a state of minimal energy. We consider here an isotropic force, proportional to $-\alpha\mathbf{v}$.

3.2 *Static Equilibrium*

Figure 1 displays the first few static equilibria, while Table 1 lists the first 18, which includes in particular the regular isocahedron for $N = 12$. Strikingly, roughly beyond this limit of about $N = 20$, there exists more than one set of equilibria for a given value of N , and the configuration of lowest energy is not necessarily the most symmetric. The overall structure is not far from hexagonal close packed, but with a radial layering.

3.2.1 *Large N limit*

Figure 3 displays both the mean mass profile and the corresponding section through $N \geq 512$ lattices; both the mass profile and the sections are derived while stacking different realisations of the lattice and binning the corresponding density. Note that the inner regions are more blurry as N increases; indeed, the inner layers are frozen early on by the infall of the outer layers.

3.2.2 *Stratification in spherical shells*

Given the number density of particles, $n(r) \equiv \rho(r)/m$, we may compute the total number of particles as

$$N = \int_0^{r_m} n(r) 4\pi r^2 dr = \frac{\pi^2}{8} n_0 r_m^3, \quad (24)$$

where $n_0 \equiv \rho_0/m$. If the stratification involves N_L layers, given that $dr/n^{-1/3}(r)$ is the fractional increase in layer number, we have

$$\int_0^{r_m} \frac{dr}{n(r)^{-1/3}} = N_L + 1/2, \quad (25)$$

(where the factor of $1/2$ accounts for the unique central particle); hence,

$$N_L = \left(\frac{\pi}{8} N\right)^{1/3} - \frac{1}{2}. \quad (26)$$

Following the same route without integrating out to the outer layer, we may ask ourselves what fraction of the radius, ξ_i corresponds to layer i ; it will obey:

$$i + 1/2 = \int_0^{r_m \xi_i} \frac{dr}{n^{-1/3}}. \quad (27)$$

Hence

$$i + 1/2 = \frac{2}{\pi} (N_L + 1/2) \left[\sin^{-1} \xi_i + x_i \sqrt{1 - \xi_i^2} \right]. \quad (28)$$

Conversely, the number of particles, $N(\leq i)$ within (and including) layer i is given by

$$N(\leq i) = \frac{2N}{\pi} \left[\frac{8}{3} (\xi_i \sqrt{1 - \xi_i^2})^3 + \sin^{-1} \xi_i - \frac{1}{2} \xi_i \sqrt{1 - \xi_i^2} \right]. \quad (29)$$

Solving the implicit Eq. (28) for the relative radius ξ_i of layer i and putting it into Eq. (29) yields the number of particles within layer i as a function its rank. The radii of the layers, $\xi_i r_m$ follows from inverting Eq. (28) for ξ_i . Examples of such shells are shown in Fig. (2).

3.3 Thermodynamics of dissolving crystal

How does the shell structure disappear as a function of temperature increase ? Fig. 4 displays the specific heat measured by the increase of quasi energy with quasi temperature in units of kN ; Here the quasi temperature is a^2 times the kinetic energy relative to the time dependant ‘‘Hubble flow’’ divided by Nk ; while the quasi energy is the sum of the quasi kinetic energy plus W_2 given by Eq. (6). During the large amplitude pulsation of the system, the quasi energy that is shared between the different components in the statistical equilibrium. Since W_2 is only repulsive, the system displays characteristics similar to a hard sphere gas. Hence there is no latent heat as there are no bonds and therefore no bonds to break.

4 Conclusion

In this paper, we demonstrated that very special systems, those for which the oscillation of the system separates off dynamically from the behaviour of the rescaled variables, can form solids (abeit ones that pulsate in scale). We

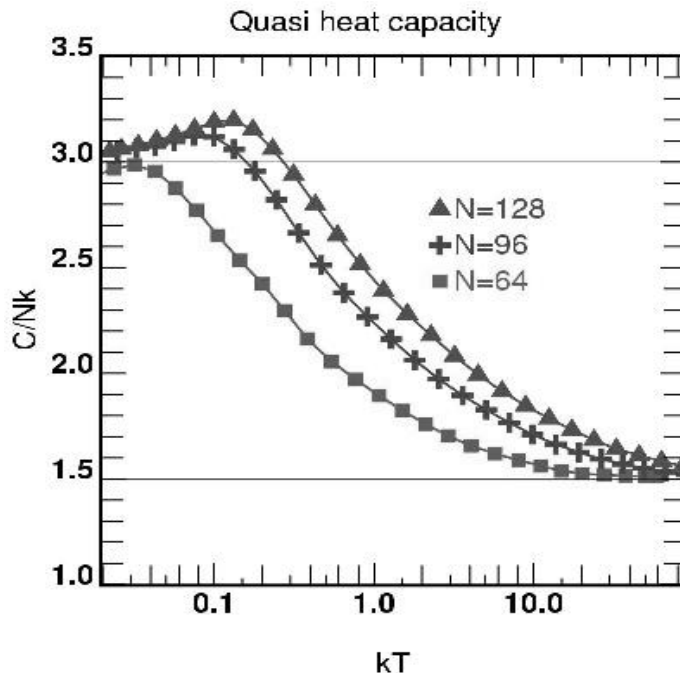


Fig. 4. quasi specific heat measured by increase of quasi energy with quasi temperature in units of kN ; the quasi temperature is a^2 times the kinetic energy relative to the time dependant “Hubble flow”, $a(t)$, divided by Nk ; the quasi energy is the sum of the quasi kinetic energy plus W_2 ; W_2 is a^2 times the repulsive part of the potential energy. During the large amplitude pulsation of the system, the quasi energy is conserved. It is the quasi energy that is shared between the different components in the statistical equilibrium. Since W_2 is only repulsive, the system displays characteristics similar to a hard sphere gas. Hence there is no latent heat as there are no bonds and therefore no bonds to break. There is a continuous transition between the cold crystal lattice and the “free” gas.

studied their phase transition and the corresponding quasi “specific heat” as these structures melt. As expected, we found that the heat capacity half to that of a free gas, but the phase transition appears to occur gradually even at large N . Although we expected a set or regular and semi regular solids, which we did find for small N , and an hexagonal close packing of most of the system at larger N , we did not foresee the strong shell structure found. Nevertheless, we constructed a theory that explained this shell structure once it had been recognized. Another by-product of our study was that the internal energy of the corresponding barotropic gas scales as $\rho^{\gamma-1}$, *i.e.* as $(\text{scale})^{-3(\gamma-1)}$ so that for $\gamma = 5/3$, it scales like $(\text{scale})^{-2}$. Thus our investigation applies equally to a $\gamma^{5/3}$ gas with a quasi gravity such that every element of fluid attract every other in proportion to their separation. It is well known, since Newton, that such attractions are equivalent to every particle being attracted in proportion to its distance to the centre of mass as though the partial mass were concentrated there. Recently Price & Monaghan (2006) used simulations of such systems to test their smooth particle hydrodynamic codes without

knowledge of its connection to the N-body problem discussed here.

Java animations describing the both the static and the pulsating and rotating crystals are found at <http://www2.iap.fr/users/pichon/spin.html> and <http://www2.iap.fr/users/pichon/lattice.html>. In Lynden-Bell (2006) a discussion of such rotating configurations is given and the analogous gaseous model is also extended to rotating fluids.

Acknowledgements *We thank Prof Ruth Lynden-Bell for discussions and David Wales for verifying our structures with his more thorough and well tested program. We also thank J. Pichon for his help. We would like to thank D. Munro for freely distributing his Yorick programming language (available at <http://www.maumae.net/yorick/doc/index.html>) which we used to implement our N-body program.*

References

- Arad I., Lynden-Bell D., 2005, MNRAS, 361, 385
Bogdan, T.V. & Wales, D.J., J.Chem Phys 120, 11090
Binney J., 2004, MNRAS, 350, 939
Eddington A. S., 1916, MNRAS, 76, 572
Lynden-Bell, D. 1967 MNRAS 136, 101
Lynden-Bell D., 1967, MSRSL, 55, 143
Lynden-Bell D., Lynden-Bell R. M., 1977, MNRAS, 181, 405
Lynden-Bell D., 1999, PhyA, 263, 293
Lynden-Bell, D. & Lynden-Bell, R.M. 1999 Proc R Soc A 455, 475 Paper I
Lynden-Bell, D. & Lynden-Bell, R.M. 1999 Proc R Soc A 455, 3261 Paper II
Lynden-Bell, D. & Lynden-Bell, R.M. 2004 J Stat Phys 117, 199 Paper III
Lynden-Bell, D, Pichon, J. and Pichon, C. in preparation for MNRAS
Lynden-Bell D., Wood R., 1968, MNRAS, 138, 495
Price D.J. Monaghan J. J., MNRAS 365 (2006) 991-1006
Thirring W., 1970, Essais in physics 4
Wales D.J. 2001 Science 293, 2067